Solid Freeform Fabrication 2023: Proceedings of the 34th Annual International Solid Freeform Fabrication Symposium – An Additive Manufacturing Conference
Reviewed Paper

Laser beam shape optimization: Exploring alternative profiles to Gaussian-shaped laser beams in powder bed fusion of metals

Vijaya Holla[1], Philipp Kopp[1], Jonas Grünewald[2], Patrick M. Praegla[3], Christoph Meier[3], Katrin Wudy[2], Stefan Kollmannsberger[1]

[1]Chair of Computational Modeling and Simulation, Technical University of Munich,
[2]Professorship of Laser-based Additive Manufacturing, Technical University of Munich,
[3]Institute for Computational Mechanics, Technical University of Munich,

Abstract

Laser-based powder bed fusion of metals (PBF-LB/M) commonly utilizes Gaussian-shaped laser beams characterized by a high intensity at the center. However, this type of profile leads to localized high temperatures and temperature gradients. When the laser power is increased beyond a certain threshold, the temperature inside the melt pool can reach the boiling point, causing excessive metal evaporation, hydrodynamic instabilities, and undesired effects such as keyholing. On the other hand, ring-shaped laser beams generate a more uniform temperature distribution but tend to produce shallower, wider, and shorter melt pools with reduced resolution compared to the Gaussian profiles. The deep, narrow, and elongated melt pools generated by the Gaussian shapes still have advantages for increased precision in the PBF-LB/M processes. This contribution uses numerical optimization to generate a new laser beam shape that also leads to a deep, narrow, and elongated melt pool, similar to a Gaussian-shaped beam, while maintaining a lower and more uniform temperature distribution inside the melt pool. The resulting optimized laser profile lowers the maximum laser intensity by 40 % without decreasing the total laser power compared to the Gaussian profile. The more uniform distribution of temperature with a peak value of just above 3 000 °C indicates a conduction dominated process with less hydrodynamic and minimal evaporative effects. This is expected to reduce the associated defects and improve the process stability.

Keywords: Laser beam shaping, Beam shape optimization, Gaussian-shaped laser, Metal additive manufacturing, Powder bed fusion of metals

1. Introduction

Laser-based powder bed fusion of metals (PBF-LB/M) commonly employs Gaussian-shaped laser beams. This type of profile, as it focuses the heat input onto a small area, leads to localized high temperatures and temperature gradients. Increasing the laser power beyond a certain threshold to scan at a higher speed can result in excessive metal evaporation when the temperature inside the melt pool reaches the boiling point. This, in turn, causes hydrodynamic instabilities, leading to undesired effects such as keyholing [1, 2].

In recent years, advancements in laser optics have enabled the modulation of laser beam intensity profiles, primarily into other symmetric profiles such as ring-shaped [3, 4] and top-hat profiles [5]. Some methods even offer non-symmetric profiles [6]. These alternative profiles have demonstrated promising results in achieving more stable melt pools and expanding the process window.

Studies indicate that ring-shaped laser beams reduce defects such as spatter, keyhole porosity, and denudation zone width [7, 4]. In [8], the authors report an increase in power and speed by 43 % with similar geometric parameters of the melt track for ring-shaped profiles compared to Gaussian beam profiles.

While ring-shaped profiles generate more uniform temperature distributions, they produce relatively shallower, wider, and shorter melt pools with reduced resolution (large laser spot size) compared to Gaussian profiles [4]. The deep, narrow, and long melt pools generated by the Gaussian shapes still have advantages for increased precision during the PBF-LB/M process. Hence, the research question arises: How must a laser intensity profile be shaped to produce a melt pool similar in shape to the one resulting from a Gaussian-shaped laser but with a more homogeneous temperature distribution, ensuring a stable melt pool even at high laser powers? Iteratively redistributing the intensity distribution to determine such laser profiles using the experiments is time-consuming and may become impossible due to the large number of parameters that determine the shape of the laser. In this context, numerical methods offer a solution by not only predicting the temperature distributions for specific laser shapes but also the inverse – determining the laser shapes from a given temperature profiles or melt pool shapes.

In [9], the authors develop a computer-based laser beam shape optimization framework for PBF-LB/M. This framework utilizes adjoint-based optimization technique to attempt to find laser shapes (laser intensity distributions) that lead to a temperature distribution or melt pool that is as close as possible to a given target (desired temperature or melt pool). The current contribution uses this framework to determine a laser profile that generates a more uniform temperature distribution within a melt pool whose shape is comparable to that of a Gaussian beam.

The paper is organized as follows. Section 2 briefly outlines the optimization method and presents the model parameters used in this article. In Section 2.1, the numerical model employed to compute the temperature from the laser beam shape is introduced. Section 2.2 describes the formulation of the loss functional, and Section 2.3 discusses the gradient computation using the adjoint-state method. The results of the numerical optimization are presented in Section 3. Section 4 summarizes the paper.

2. Methods

The optimization framework presented in [9] computes a laser beam shape corresponding to a desired temperature. It first parameterizes the laser shape by a discrete set of parameters ("tuning knobs") that the algorithm can optimize. It then defines a loss functional that measures the quality of a laser beam shape by numerically simulating the resulting temperature in the part and comparing it to the user-defined target temperature. The further these two temperature fields are apart, the higher the loss functional value. Finally, the numerical optimization chooses an initial laser shape and iteratively improves it by minimizing the loss functional using the gradient-based L-BFGS-B algorithm [10] from the SciPy library [11]. At each iteration, this algorithm evaluates the loss functional and its gradient to compute an updated laser beam shape (a new parameter set).

2.1. Temperature computation: forward problem

To tailor the laser beam profile, the spatial intensity distribution, denoted by u, needs to be parametrized using a finite set of variables β, which serve as design parameters for the optimization. By employ-

ing various parametrizations, the laser shape can be constrained to a different set of shapes. For instance, axisymmetric laser shapes can be achieved by superimposing a given number of Gaussian functions, as demonstrated in [9]. In this study, to enable the laser profile to adopt any shape, the intensity is parametrized using 2 400 piecewise "hat" functions as follows:

$$u(\hat{\beta}) = \sum_i N_i(x,y)\,\hat{\beta}_i, \tag{1}$$

where N_i represents the ith shape function formed by a tensor product of two piecewise "hat" functions along x and y directions, and $\hat{\beta}_i$ corresponds to the coefficient associated with it.

The temperature is computed from the laser intensity profile using the steady-state convection-diffusion equation with non-linear coefficients. The model assumes a laser traveling over a bare metal plate with a constant intensity profile. It is assumed that the temperature near the laser evolves to a steady state. Hence, the stationary form of the heat equation is considered as follows:

$$v \cdot c\nabla T - \nabla \cdot (k\nabla T) = 0 \qquad \text{on}\,\Omega \tag{2}$$

$$k\nabla T \cdot n = \alpha u(\beta) \qquad \text{on}\,\Gamma_{N_L} \tag{3}$$

$$k\nabla T \cdot n = 0 \qquad \text{on}\,\Gamma_{N_0} \tag{4}$$

$$T(0) = T_0 \qquad \text{on}\,\Gamma_D. \tag{5}$$

In this PDE (also called the forward problem), T and ∇T represent the temperature and its gradient inside the computational domain Ω, while v denotes the laser velocity. The non-linear coefficients $c(T)$ and $k(T)$ are the temperature-dependent thermal capacity and heat conductivity, respectively. The Neumann and Dirichlet boundary conditions are applied on $\Gamma_N = \Gamma_{N_L} \cup \Gamma_{N_0}$ (top, bottom, and right boundaries of the domain shown in Figure 1) and Γ_D (left boundary of the domain shown in Figure 1, with T_0=20°C), where $\Gamma_N \cup \Gamma_D = \partial\Omega$, such that $\Gamma_N \cap \Gamma_D = \emptyset$. The laser intensity is applied as a Neumann boundary condition on the top boundary of the domain (Γ_{N_L}) with a constant absorptivity factor α. Moreover, $c(T)$ is augmented with a latent heat of fusion term, following [12, 13]:

$$c(T) = \rho c_s(T) + \rho L f'_{pc}(T). \tag{6}$$

Here, ρ represents the material density, $c_s(T)$ is the specific capacity, L is the latent heat of melting, and $f_{pc}(T)$ is a phase function that regularizes the transition between the solid (value zero) and the liquid state (value one). Its temperature derivative is denoted as $f'_{pc}(T)$.

2.2. Loss function definition

The Gaussian-shaped laser beam, when used at high laser power, generates a deep, narrow, and elongated melt pool where the temperature inside reaches the boiling point. This excessive heating indicates significant evaporation, which is not included in the mathematical model but may cause defects in reality. The temperature profile obtained from solving the heat conduction model (using Equations (2) to (5)) for the Gaussian-shaped laser beam (as shown in Figure 1(b)) exhibits maximum values well above the boiling point of steel (as seen in Figure 3(a)). Although this is an unphysical result due to the model limitations, it signifies overheating and subsequent evaporation within the melt pool.

The objective of this optimization is to determine a laser beam shape that generates a melt pool similar in shape to the one resulting from a Gaussian profile while limiting the maximum temperature to the boiling point. The boiling point of the material considered in this article (AISI 316L stainless steel) is assumed to be 2 800 °C. Outside the melt pool, the target temperature is approximated. Therefore, the optimization problem and the loss functional is formulated as follows:

$$\underset{\mathrm{u}}{\textit{minimize}}\ J(T(\beta)) = \frac{1}{2}\left(\int_{\Omega} \gamma \cdot (T(\beta) - T_{appr})^2 d\Omega + \int_{\Omega} \phi \cdot (T(\beta) - 2800)^2 d\Omega\right), \quad (7)$$

subject to constraints $Eq.\ 2$ to 5.

Here, T_{appr} (shown in Figure 1(a)) is the temperature computed from the Gaussian-shaped laser of diameter ($D4\sigma$) 200 µm and power 400 W, illustrated in Figure 1(b). The laser beam at this power is expected to generate significant evaporation within the melt pool, leading to the keyhole effect. The activation function γ selectively activates the first term in the loss functional outside the melt pool M (see Figure 1(a)). It is defined as:

$$\gamma(x,y,z) = \begin{cases} 0, & \text{if } (x,y,z) \in M \\ 1, & \text{otherwise.} \end{cases} \quad (8)$$

Similarly, ϕ activates the penalization of temperatures above 2 800 °C. It is defined as:

$$\phi(T) = \begin{cases} 1, & \text{if } T > 2800 \\ 0, & \text{otherwise.} \end{cases} \quad (9)$$

In Equation (8), the first term aims to achieve the melt pool shown in Figure 1(a). The second term constrains the maximum temperature to be less than the boiling point of stainless steel to prevent overheating and evaporation.

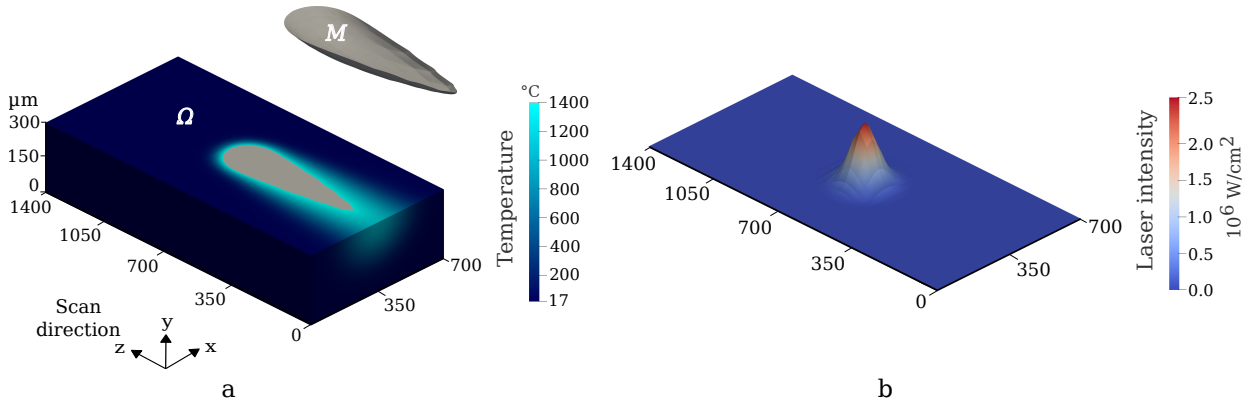

Figure 1: (a) Target (desired) temperature and melt pool, (b) Gaussian-shaped laser beam that is used to generate (a).

2.3. Gradient computation: adjoint problem

To compute the gradient using the adjoint-state method, an additional field called the adjoint field, denoted as λ, is introduced. It is computed by solving the following adjoint-state equation (also called the adjoint problem), given by:

$$v \cdot (c + c'T)\nabla\lambda + \nabla \cdot (k + k'T)\nabla\lambda = f_{adj} \qquad \text{on } \Omega \tag{10}$$

$$v \cdot (c + c'T)n\lambda + (k + k'T)\nabla\lambda \cdot n = 0 \qquad \text{on } \Gamma_N \tag{11}$$

$$\lambda(0) = 0 \qquad \text{on } \Gamma_D, \tag{12}$$

$$\text{where} \quad c' = \frac{\mathrm{d}c}{\mathrm{d}T} \quad \text{and} \quad k' = \frac{\mathrm{d}k}{\mathrm{d}T}. \tag{13}$$

Here, the coefficients c, c', k, and k' are dependent on the temperature T, the solution to the forward problem. In eq. (10), f_{adj} is the adjoint source term and is computed by taking the derivative of the loss functional with respect to the temperature:

$$f_{adj} = \gamma \cdot (T(\beta) - T_{appr}) + \phi(T) \cdot (T(\beta) - 2800). \tag{14}$$

Finally, the gradient of the loss functional with respect to the laser intensity parameters is calculated using the following equation:

$$\frac{\partial J}{\partial \hat{\beta}_i} = \int_{\Gamma_{N_L}} \lambda N_i \, \mathrm{d}\Gamma_{N_L}. \tag{15}$$

Here, $\partial J / \partial \hat{\beta}_i$ is the gradient of the loss functional with respect to ith coefficient $\hat{u}_i$. More details about the adjoint-state method and the gradient computation for laser beam shape optimization in PBF-LB/M can be found in [9].

2.4. Model parameters

For all numerical studies, a domain of size $1\,400 \times 700 \times 300\,\mu\mathrm{m}$ is considered. The domain size is chosen to be sufficiently larger than the target melt pool shapes to minimize the influence of the boundaries on the results. A laser velocity of $800\,\mathrm{mm/s}$ is considered. Hexahedral finite elements with multi-level hp-refinement from [14] are used for all simulations. The material used for the model is AISI 316L stainless steel. The material and model properties are given in Table 1.

Material and Phase change parameters	
Laser absorptivity (α)	0.3
Specific heat capacity at $0\,^\circ\mathrm{C}$ ($c_s(0\,^\circ\mathrm{C})$)	$472\,\mathrm{J/kg\,^\circ C}$
Temperature derivative of c_s (c_s')	$101.02 \times 10^{-3}\,\mathrm{J/kg}$
Conductivity at $0\,^\circ\mathrm{C}$ ($k(0\,^\circ\mathrm{C})$)	$13.6\,\mathrm{W/m\,^\circ C}$
Temperature derivative of k (k')	$15.3 \times 10^{-3}\,\mathrm{W/m}$
Density (ρ)	$7\,984\,\mathrm{kg/m^3}$
Latent heat (L)	$2.8 \times 10^5\,\mathrm{J/kg}$

Table 1: Material and Model parameters.

3. Results and Discussion

This section presents the numerical results obtained from the optimization. The optimization process consisted of a total of 77 L-BFGS-B iterations, resulting in a reduction of the loss value to 0.25 % of its initial value. The termination condition for the optimization was met when the relative change in the loss functional reached below the threshold of 2.22×10^{-9}. Each iteration required approximately 180 s to solve the forward problem with 35 000 unknowns and the adjoint problem with 110 00 unknowns per finite element computation on a 2.6 GHz Intel Core i7-10750H machine. Following the optimization, the laser profile was post-processed to remove spurious negative intensities by replacing them with zero and scaling down the positive intensities to match the integrated laser power of the original optimization result. Subsequently, the corresponding temperature profile and melt pool for the post-processed laser profile were computed by solving the forward problem.

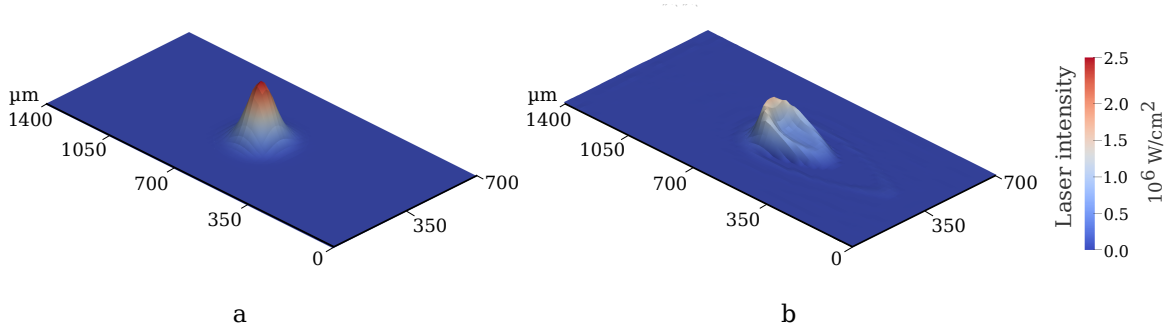

Figure 2: (a) Gaussian-shaped laser beam that is used to generate Figure 1(a), (b) Optimized laser beam shape.

Figure 2 compares the Gaussian-shaped laser beam in (a), corresponding to the target (desired) melt pool, to the optimized laser intensity profile in (b). The Gaussian-shaped laser beam has a power of 400 W with a maximum intensity value of $2.62\,\mathrm{MW/cm^2}$. In contrast, the optimized profile features a distinctive c-shaped intensity distribution with a power of 392 W and a maximum intensity value of $1.58\,\mathrm{MW/cm^2}$, which is 40 % lower than the Gaussian profile. Thus, the profile is improved without changing the laser power substantially.

Figure 3 illustrates the corresponding temperature distributions and melt pools for the Gaussian-shaped profile in (a) and the optimized intensity profile in (b). The optimized laser beam generates a melt pool that closely resembles the target melt pool, achieved through the first term in the loss functional given in Equation (8). However, the depth is reduced by 18 %, and the volume of the melt pool is reduced by 11 %, measuring $2.5 \times 10^{-6}\,\mathrm{cm^3}$, compared to the target melt pool volume of $2.8 \times 10^{-6}\,\mathrm{cm^3}$. By incorporating the second term in the loss functional, the optimization yielded the intensity distribution that generates a more homogeneous distribution of energy, thereby restricting the maximum temperature to 3 113 °C (see Figure 3(c)). Although this value slightly exceeds the target temperature of 2 800 °C, it is a significant improvement compared to the Gaussian-shaped laser, which concentrates the energy at the center and raises the temperature to 5 926 °C which indicates strong evaporation and melt pool dynamics due to the excessive heat.

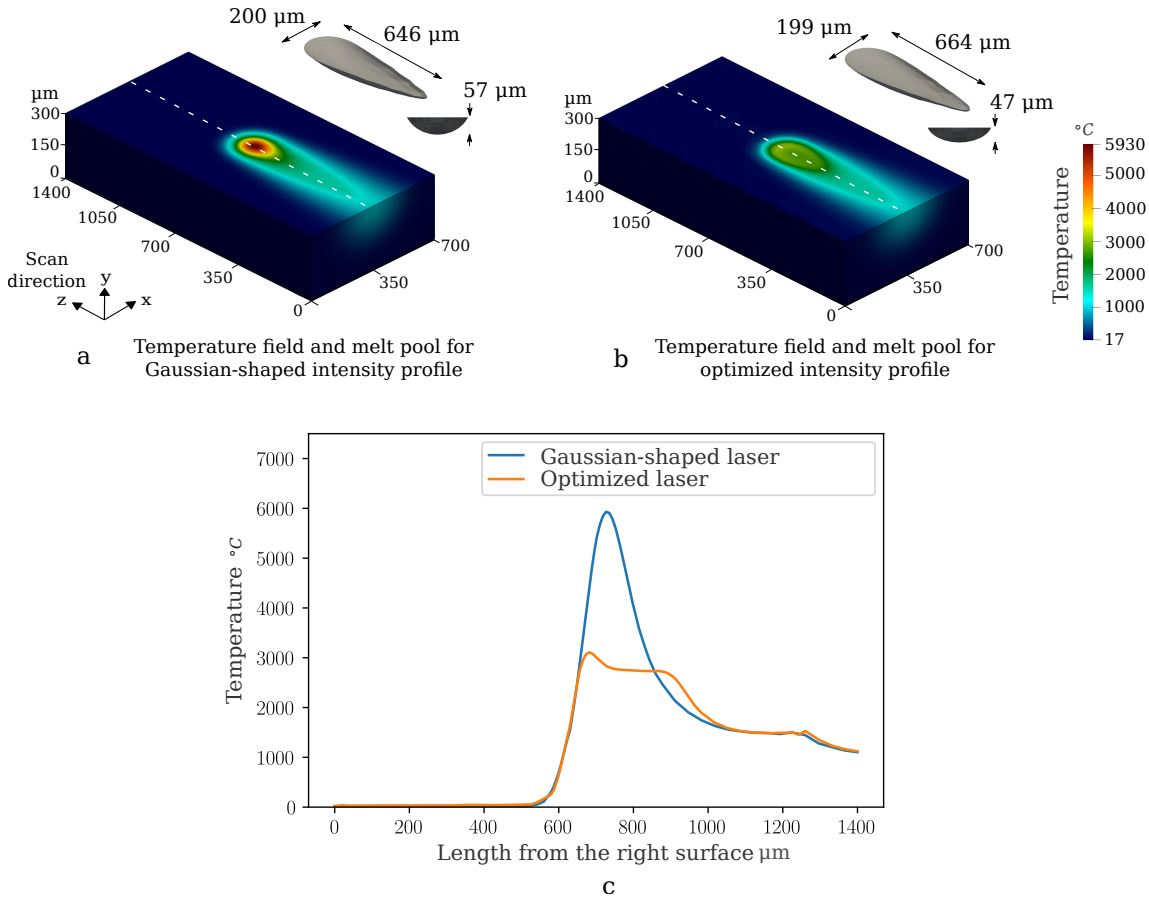

Figure 3: (a) Temperature distribution and the target melt pool corresponding to the Gaussian-shaped laser beam, (b) Temperature distribution and melt pool corresponding to the optimized laser beam shape, (c) Temperature profile plotted along the scan direction corresponding to the Gaussian-shaped laser and the optimized laser.

4. Conclusion

In this study, we employ the laser beam shape optimization framework presented in [9] to find a laser profile alternative to the Gaussian-shaped profile, demonstrating the potential of the framework for computing unique laser shapes tailored to specific applications. This alternative produces a melt pool which is similar in shape, yet exhibits a lower maximum temperature within the melt pool. The optimization is carried out by formulating a loss functional that aims to generate a deep, narrow, and elongated melt pool similar to the Gaussian-shaped laser beam. Additionally, to achieve a more stable melt pool, the loss functional penalizes the temperatures exceeding the boiling point of Stainless steel 316L. To introduce greater flexibility into the laser shape, the intensity is parametrized using 2 400 piecewise “hat” functions. The resulting optimized laser beam shows a c-shaped profile, with a 40 % reduction in the maximum intensity compared to the Gaussian shape. Consequently, this laser profile generates a more uniform temperature distribution within the melt

pool, with the maximum temperature reaching 3 113 °C, in contrast to the 5 926 °C maximum temperature produced by the Gaussian-shaped laser. The resulting melt pool has a similar shape to the melt pool corresponding to the Gaussian-shaped laser beam. However, the melt pool depth and volume are reduced by 18 % and 11 %, respectively. Future work will investigate the influence of these laser profiles on the melt pool dynamics at high laser power through experimental studies.

Acknowledgement

We gratefully acknowledge the support of Deutsche Forschungsgemeinschaft (DFG, German Research Foundation) through the grant KO 4570/2-1.

References

[1] I. Yadroitsev, I. Yadroitsava, A step-by-step guide to the l-pbf process, in: Fundamentals of Laser Powder Bed Fusion of Metals, Elsevier, 2021, pp. 39–77.

[2] R. Cunningham, C. Zhao, N. Parab, C. Kantzos, J. Pauza, K. Fezzaa, T. Sun, A. D. Rollett, Keyhole threshold and morphology in laser melting revealed by ultrahigh-speed x-ray imaging, Science 363 (2019) 849–852.

[3] T. M. Wischeropp, H. Tarhini, C. Emmelmann, Influence of laser beam profile on the selective laser melting process of alsi10mg, Journal of Laser Applications 32 (2020) 022059.

[4] J. Grünewald, F. Gehringer, M. Schmöller, K. Wudy, Influence of Ring-Shaped Beam Profiles on Process Stability and Productivity in Laser-Based Powder Bed Fusion of AISI 316L, Metals 11 (2021) 1989.

[5] I. V. Zhirnov, P. A. Podrabinnik, A. A. Okunkova, A. V. Gusarov, Laser beam profiling: experimental study of its influence on single-track formation by selective laser melting, Mechanics & Industry 16 (2015) 709.

[6] J. Grünewald, V. Blickle, M. Allenberg-Rabe, P. Wagenblast, K. Wudy, Flexible and highly dynamic beam shaping for laser-based powder bed fusion of metals, Procedia CIRP 111 (2022) 65–70.

[7] M. Rasch, C. Roider, S. Kohl, J. Strauß, N. Maurer, K. Y. Nagulin, M. Schmidt, Shaped laser beam profiles for heat conduction welding of aluminium-copper alloys, Optics and Lasers in Engineering 115 (2019) 179–189.

[8] A. S. Metel, M. M. Stebulyanin, S. V. Fedorov, A. A. Okunkova, Power density distribution for laser additive manufacturing (slm): potential, fundamentals and advanced applications, Technologies 7 (2018) 5.

[9] V. Holla, P. Kopp, J. Grünewald, K. Wudy, S. Kollmannsberger, Laser beam shape optimization in powder bed fusion of metals, Additive Manufacturing (2023) 103609.

[10] R. H. Byrd, P. Lu, J. Nocedal, C. Zhu, A limited memory algorithm for bound constrained optimization, SIAM Journal on scientific computing 16 (1995) 1190–1208.

[11] P. Virtanen, R. Gommers, T. E. Oliphant, M. Haberland, T. Reddy, D. Cournapeau, E. Burovski, P. Peterson, W. Weckesser, J. Bright, et al., Scipy 1.0: fundamental algorithms for scientific computing in python, Nature methods 17 (2020) 261–272.

[12] P. Kopp, V. Calo, E. Rank, S. Kollmannsberger, Space-time hp-finite elements for heat evolution in laser powder bed fusion additive manufacturing, Engineering with Computers (2022) 1–15.

[13] S. Kollmannsberger, A. Özcan, M. Carraturo, N. Zander, E. Rank, A hierarchical computational model for moving thermal loads and phase changes with applications to selective laser melting, Computers & Mathematics with Applications 75 (2018) 1483–1497.

[14] P. Kopp, E. Rank, V. M. Calo, S. Kollmannsberger, Efficient multi-level hp-finite elements in arbitrary dimensions, Computer Methods in Applied Mechanics and Engineering 401 (2022) 115575.